Nanoscale

RSC Publishing

PAPER

View Article Online
View Journal | View Issue



Cite this: *Nanoscale*, 2013, **5**, 10550

# Coupled plasmons induce broadband circular dichroism in patternable films of silver nanoparticles with chiral ligands†

Xavier Vidal,[ab] Won Jin Kim,[a] Alexander Baev,[a] Valentyna Tokar,[ac] Hongsub Jee,[a] Mark. T. Swihart[ad] and Paras N. Prasad*[aefg]

This contribution reports the chiro-optic response of as-cast and photopatterned films of silver nanoparticles capped with photothermally-cleavable chiral ligands. We demonstrate broadband circular dichroism in these nanoparticle films, which is not present in dispersions of the nanoparticles capped with the chiral ligands. Long wavelength circular dichroism is derived from coupling of the plasmonic bands of neighbouring silver nanoparticles. Furthermore, the chiral response is preserved in the microstructured film after photopatterning using direct two-photon absorption in the plasmonic band of the silver nanoparticles. Thus, both the as-cast and photopatterned films show circular dichroism from the UV wavelength of intrinsic absorption of the ligand, through the plasmon resonances of both the isolated silver nanoparticles and the interacting nanoparticles, which extend to the near IR. Density functional theory (DFT) calculations of model electronic complexes of a chiral ligand and a small metallic cluster suggest that the new chiral bands at the plasmonic resonances are derived from new chiral hybrid electronic states of the metal nanoparticle–ligand complexes.

Received 24th June 2013
Accepted 31st August 2013

DOI: 10.1039/c3nr03244b

**www.rsc.org/nanoscale**

## Introduction

Chiral optically-active nanoparticles (NPs) can be a key building block for future nanotechnology. Chirality has particular importance in nanotechnology–biotechnology interactions, as biological processes are based on self-assembly of molecules dominated by homochirality.[1] Optimal future development of nanoscience and nanotechnology requires control and understanding of discrete nano-elements, their interactions, and their coupling to surrounding media.[2] In this work, we analysed the optical activity of Ag NPs with chiral ligands, focusing on the evolution of the chiro-optical response from the dispersed NPs, to the final patterned nanostructured films. The plasmonic NPs were functionalized with thermally-labile chiral ligands, then patterned with two-photon lithography driven by direct two-photon absorption at the localized surface plasmon resonance (LSPR) wavelength of the Ag NPs. Functionalization of NPs is crucial for controlling their interactions with one another and with their surroundings. The Ag NPs with chiral ligands are the minimal effective entity for producing optical activity.[3] Because of the high surface to volume ratio of nanoparticles, modification of their surfaces can have a major impact on their properties, including their optical response.[4,5] Metallic NPs (MNP) are an effective tool for enhancement and control of optical effects due to their LSPR and associated local enhancement of electromagnetic fields.[6–10] This tightly confined electromagnetic field decays exponentially away from the metal surface, resulting in an evanescent wave; thus, the distance between MNPs plays an important role in tuning interactions between nanoparticles and the collective plasmon resonances in NP assemblies. The interaction among the NPs can enhance the LSPR and the optical effects that depend on it. Such plasmon-induced enhancement is influenced by the specific modification or functionalization of the MNPs, which can be strategically selected to meet the specific requirements for each application. In fact, several recent papers have demonstrated plasmonic enhancement of optical effects[11] including optical circular dichroism (CD), showing that achiral metallic particles with chiral organic ligands can exhibit chiral response at the plasmon frequency.[12–15] Gautier and Bürgi showed the importance of the ligand in the optical activity of MNPs.[16] This response is

[a]*Institute for Lasers, Photonics and Biophotonics, University at Buffalo, The State University of New York, Buffalo, New York, 14260, USA*

[b]*Department of Physics and Astronomy, Macquarie University, New South Wales, 2109, Australia. E-mail: xavier.vidal@mq.edu.au; Fax: +61 298508115; Tel: +61 298506368*

[c]*Faculty of Physics, Taras Shevchenko National University of Kyiv, 64 Volodymyrska st., Kyiv, 01601, Ukraine*

[d]*Department of Chemical and Biological Engineering, University at Buffalo, The State University of New York, Buffalo, New York, 14260, USA. E-mail: swihart@buffalo.edu*

[e]*Department of Chemistry, University at Buffalo, State University of New York, Buffalo, New York, 14260, USA. E-mail: pnprasad@buffalo.edu*

[f]*Department of Electrical Engineering, University at Buffalo, State University of New York, Buffalo, New York, 14260, USA*

[g]*Department of Chemistry, Korea University, South Korea*

† Electronic supplementary information (ESI) available. See DOI: 10.1039/c3nr03244b

attributed to coupling of surface plasmons of individual MNPs with chiral molecules. In assemblies of MNPs, this enhancement can be boosted by judiciously controlling interparticle distance. This distance determines the near-field interaction between neighboring MNPs and thus their ability to create collective surface plasmon resonances.[17,18] Hentschel *et al.*, for example, reported that artificial structures with molecular configurations showed tailorable collective surface plasmon resonances.[19] In that case, gold NPs play the role of monomers, whose interparticle separation was gradually changed, showing the transition from isolated to collective modes. Shen and coworkers have also demonstrated a plasmonic absorption enhancement in organic solar cell devices by controlling the distance between MNPs to maximize their near-field interactions.[20] Although LSPR-induced enhancements have been intensively studied, few practical studies have been devoted to the possible applications of collective surface plasmons using MNP assemblies.[21] One example is the collective plasmon–plasmon interaction of MNPs in a helical arrangement.[22] The preservation of the optical properties of a medium after photolithographic patterning can be of key importance for many practical applications.[23–25] As an example, maintaining the chirality of building blocks is crucial, if a planar chiral metamaterial is to be fabricated by photopatterning of those building blocks. In this case, the resulting optical activity of the material can be greatly enhanced. Therefore, another potential application of such patterns is to study enhanced circular dichroism.[25]

## Results and discussion

Here, we show an enhancement of optical activity of MNPs with chiral ligands, after being photopatterned as described previously in ref. 26. We demonstrate that ligand-induced chirality of MNPs is preserved in the fabricated patterns. Several groups have recently utilized two-photon lithography for the patterning of solid state films by *in situ* growth of MNPs in a polymer matrix.[27–30] However, this approach results in limited loading of MNPs in the patterned area. Furthermore, optical properties of *in situ* grown MNPs are very difficult to control in a reliable and reproducible fashion. The MNPs may lose their individual properties (*e.g.* LSPR) as they sinter into structures closer to the bulk metal. For this reason, in the present work, we have photopatterned Ag NPs without any host material. We have previously demonstrated that NPs modified with a ligand containing a labile *t*-butoxycarbonyl (*t*-BOC) group[31] can be photopatterned.[26] The *t*-BOC protected ligand is readily activated and deprotected photothermally, driven by nonlinear (two-photon) LSPR absorption. Deprotection of the ligands dramatically reduces the dispersibility of the nanocrystals, enabling a solvent-selective development process after photopatterning. Ag NPs were prepared using established procedures.[32] The dodecanoic acid ligands used in the synthesis, or other *in situ* generated ligands, were replaced with *N*-(*tert*-butoxycarbonyl)-L-cysteine methyl ester. The resulting *t*-BOC protected Ag NPs were examined by transmission electron microscopy (TEM, Fig. 1a) which showed spherical Ag NPs with a mean diameter of

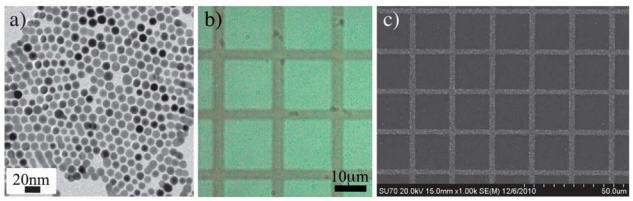


**Fig. 1** (a) TEM image of Ag NPs, (b) optical and (c) SEM image of two-photon patterned Ag NP films.

$9.3 \pm 0.9$ nm. Films of 150 nm thickness were obtained by spin coating onto a glass or quartz substrate from a 45 mg $ml^{-1}$ dispersion of Ag NPs in chloroform. The photopatterns were made as previously reported.[26] Briefly, under femtosecond pulsed laser irradiation at 800 nm, the silver nanoparticles in the film are excited through two-photon absorption, which is particularly strong because the LSPR frequency of the silver nanoparticles (~400 nm) is matched to two 800 nm photons. The two-photon absorption heats the Ag NPs, initiating thermal decomposition of the ligands, resulting in a shortening of the chiral ligand. The written patterns were developed using chloroform–ethanol (4 : 1, v/v) (Fig. 1b and c).

To understand deprotection of ligands on Ag NPs by photothermal reaction, we used Fourier Transform Infrared (FT-IR) spectroscopy to probe the chemical structure change on the surface of the Ag NP. The FT-IR studies were conducted at room temperature. A sodium chloride (NaCl) disk IR flow cell was used as a blank upon which the sample of dispersed Ag NPs in chloroform was drop-casted. After recording the IR spectra of *t*-BOC protected Ag NPs, the film was exposed to laser illumination using the same method as described for the two-photon lithography to obtain *t*-BOC deprotected Ag NPs. As shown previously in Kim *et al.*[26] the expected significant changes are in the peaks corresponding to the carbonyl, methyl and amine groups at 1702 $cm^{-1}$, 2975 $cm^{-1}$ and around 3350 $cm^{-1}$, respectively. Specifically, the strong carbonyl stretching peak is drastically decreased after deprotection of the *t*-BOC moiety, suggesting that the *t*-BOC groups are selectively deprotected through the photothermal reaction. This effect is stronger at the methyl stretching peak, which is drastically decreased. However, no significant change is present in the amine group when the MNPs were patterned by LSPR-induced photothermal lithography.

Prior to photopatterning, the Ag NPs properties were analyzed *via* UV-vis absorbance and CD spectroscopy in solution. Fig. 2a shows the absorption spectrum of the surface plasmon resonance band. The expected LSPR absorption is present at 410 nm for particles dispersed in chloroform. The resonance is red-shifted and broadened in the film. The broadening and shift of the plasmonic band is a result of the interaction among closely spaced MNPs.[33] Fig. 2b shows the CD response of the same solution. Along with the molecular CD at UV frequencies, significant CD response at longer wavelengths, near the LSPR frequency is also observed. This longer wavelength response arises from the hybridization between the achiral Ag NPs and their chiral ligands.[34]

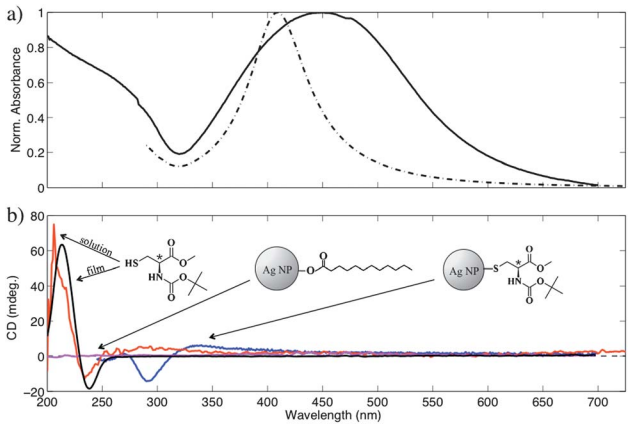


**Fig. 2** (a) Absorption spectra of *t*-BOC Ag NP film (solid line) and dispersion in chloroform (dotted line); (b) CD spectra of *N*-(*tert*-butoxycarbonyl)-L-cysteine methyl ester dissolved in ethanol (red line), and as a film (black line), dodecanoic acid protected Ag NPs (as a film, magenta line), and *t*-BOC protected Ag NPs dispersed in chloroform (blue line).

To better understand the origin of the red-shifted LSPR absorbance that arises from near-field coupling of silver NPs in the film, we simulated the absorbance spectra of various small chains and clusters of silver nanoparticles, as shown in Fig. 3. Simulations were conducted using the finite element-based (FE) COMSOL multiphysics RF solver using a time-harmonic approximation (http://www.comsol.com). The dielectric constant of silver was represented by the usual Drude dispersion curve. As shown in Fig. 3, each specific cluster or chain of particles produces one or more distinct red-shifted absorbance peaks. The peak position depends upon the arrangement of the particles in the cluster. In the random packing of nanoparticles

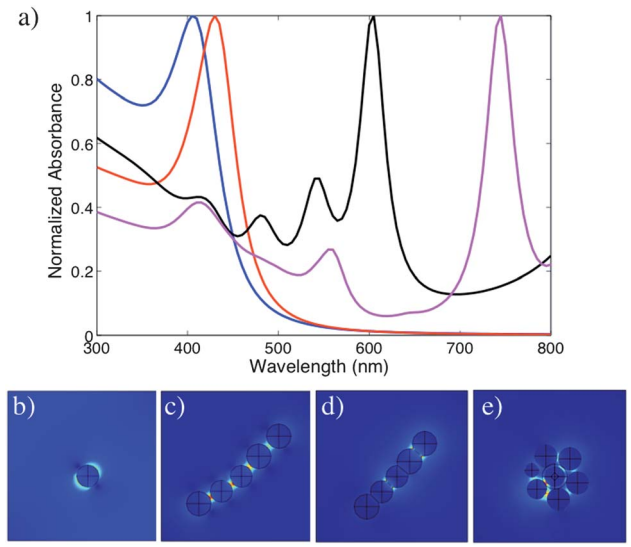


**Fig. 3** (a) Normalized absorbance spectra of an isolated silver nanoparticle (10 nm size) and different configurations of Ag NPs clusters: single Ag NP (blue line), chain of 5 Ag NPs (red line), cluster of 5 Ag NPs (black line), and cluster of 9 Ag NPs (magenta line); (b)–(e) cross-sectional plots of the norm of the electric field at $z = 0$. In each case (b though e) the wavelength corresponds to the maximum value of absorbance.

that is presumably present in the particle films, this results in a single broad peak that arises from the superposition of many spectra like those illustrated in Fig. 3a. The maps of the norm of the electric field within these clusters, shown in Fig. 3(b) through (e), illustrate the local field enhancement produced within the clusters of plasmonic nanoparticles, particularly in the spaces between particles.

To investigate LSPR-induced optical chiral response, the *t*-BOC protected Ag NP solutions were drop-cast onto a quartz plate and CD spectra were recorded at room temperature. We confirmed that the studied films had the same thickness by measuring the absorbance of all samples before taking CD spectra. The CD response of the Ag NP films was studied prior to lithographic patterning. In the film, new CD bands appear at longer wavelengths, which were not observed for the particles in solution. As a control, note that a film of (achiral) dodecanoic acid protected Ag NPs does not show any CD response (Fig. 2b). No significant differences were observed between the CD spectra of *N*-(*tert*-butoxycarbonyl)-L-cysteine methyl ester in solution or as a film (Fig. 2b). The film of *t*-BOC protected Ag NPs shows a CD response close to the LSPR absorbance band induced by the interaction of the Ag NPs with their chiral ligands, at wavelengths below 450 nm (Fig. 4), as anticipated from the CD in solution. In addition, new characteristic CD responses were observed in the range of 450–800 nm (Fig. 4), as a consequence of the interaction among Ag NPs. This is a result of the close packing of NPs, which introduces new CD bands because of the collective plasmonic excitations[19] of coupled Ag NPs interacting with their chiral ligands. Interestingly, the appearance of new LSPR absorbance bands has been shown with a simple pair of Ag NPs.[35] Thus, the spin-coated film shows a molecular CD at UV frequencies from the chiral ligands, plasmon-induced CD at UV-visible frequencies due to the coupling of surface plasmons of individual MNPs with the chiral molecules and collective plasmon-induced CD at visible to near infrared wavelengths, arising from interactions among the closely-packed Ag NPs.

After photothermal deprotection, the CD band corresponding to the interaction of the functional chiral ligands with the individual MNPs, at 425 nm and below, is preserved. Likewise,

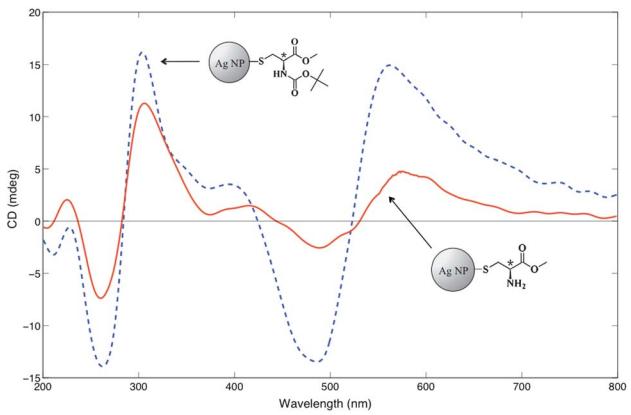


**Fig. 4** Representative CD spectra of *t*-BOC protected Ag NP film (blue line), and *t*-BOC deprotected Ag NP film (red line).

the chirality at longer wavelengths induced by the collective plasmons is maintained. The shortened ligand retains its stereospecific-structure, which is the origin of the chiral optical activity. The CD intensity is reduced due to the fact that part of the material is removed after photopatterning and developing. If the enhanced CD were mainly due to the presence of chiral ligands in "hot spots" at junctions between silver nanoparticles, one might expect it to increase after patterning, because of reduced average interparticle spacing. However, that was not the case; the effect of simply having less material remaining after patterning is dominant here. This approach differs from the one described by Abdulrahman *et al.*[36] in which achiral metallic structures show chirality induced by a surrounding chiral medium. There, the far field interaction induces chirality beyond the molecular chiral wavelength. However, our theoretical analysis presented below suggests that this mechanism is not dominant in the present case.

Optical activity can also be considered in terms of the absorption dissymmetry ratio, defined as $2(A_L - A_R)/(A_L + A_R)$, where $A_L$ and $A_R$ are the absorbencies of left and right circularly polarized light, respectively. In this case, the spectrum of dissymmetry ratio (Fig. 5) does not differ dramatically from the CD spectrum. This reflects the fact that the absorbance of the films is rather broad, and is very similar for the patterned and unpatterned films shown in Fig. S1.† The decrease in dissymmetry ratio after patterning is therefore attributed to changes in the local environment, and not simply reduction of the amount of material present. Simply removing material would not change the dissymmetry ratio. From one side the shortened ligand may potentially imply a slightly reduction of the average distance among Ag NPs, which is compensated by changes in the ratio of chiral organic material to metal nanoparticles, and the film thickness. Nonetheless, the majority of the CD remains in the patterned film.

Govorov *et al.*[37] worked out a semi-classical model of an achiral nanocrystal interacting with a chiral molecule. They concluded that the chiral currents induced in the metal nanoparticles through the dipole–dipole exciton–plasmon interaction are responsible for the appearance of new chiral bands in the CD spectrum of a particle–molecule complex, including a band at the plasmon frequency. However, they found that strong dipole–dipole exciton–plasmon interaction requires NPs of relatively large size – up to 40 nm for a single particle, and up to 20 nm for a dimer.[38] The magnitude of the signal at the plasmon frequency in the latter case strongly depends on the interparticle distance. Beyond 2 nm separation, it decreases steeply.[38] Ha *et al.*[39] related the new bands to the chiral electronic states of metal NPs, originating from adsorption of chiral ligands on the surface of NPs. In our experiments, we used relatively small NPs with the average size of 9.3 nm with chiral ligands adsorbed on their surface. The particles used here are large enough to exhibit plasmon resonance, and thus such dipole–dipole interactions can contribute to the observed total CD. The films are in an intermediate regime where both coupled hybridized ligand/particle states and induced chiral currents because of the Coulomb dipole–dipole coupling can lead to the chiroptical response.[40] Hybridization of cluster states with the states of the chiral ligand can also result in optical activity. A similar mechanism can also lead to the gigantic enhancement of molecular nonlinearities.[41] Increasing the size of the cluster results in the increased density of states and, eventually, formation of quasi-continuous energy bands. At some point plasmonic effects will come into play and the Coulomb interaction between plasmonic modes and molecular dipoles will start contributing to the observed CD. To assess the effect of chiral adsorbates on the overall CD response of the NP–ligand complex, we performed a series of DFT quantum chemical calculations of two model electronic complexes: protected and deprotected cysteine ester covalently bound to one of the vertices of a tetrahedral $Ag_{20}$ cluster (V-complex, inset Fig. 6). The tetrahedral $Ag_{20}$ cluster played the role of the Ag NPs in these calculations. As pointed out by Schatz *et al.*,[42] due to the small size of the cluster, collective excitation of electrons is inhibited. Nevertheless, the cluster can be considered as a microscopic analogue of a Ag NP. The computations were performed with the Amsterdam Density Functional (ADF) package, (ADF 2009.01, SCM Corp.) at the Density Functional (DFT) level employing the PBE[43] non-hybrid generalized gradient approximation (GGA) functional. Protected and deprotected cysteine ester geometries were optimized at the PM3 level of theory. An

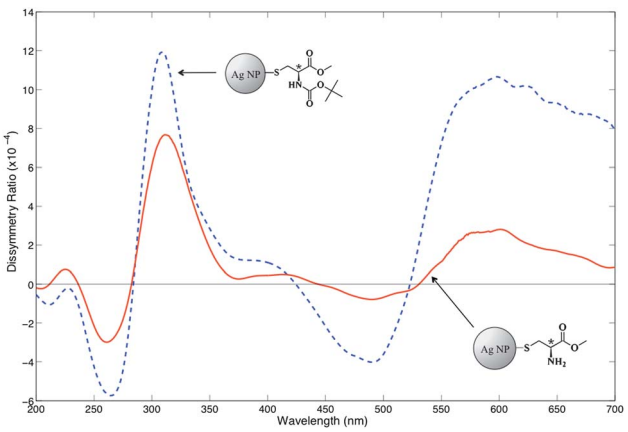


**Fig. 5** Absorbance dissymmetry ratio of *t*-BOC protected Ag NP film (blue line), and *t*-BOC deprotected Ag NP film (red line).

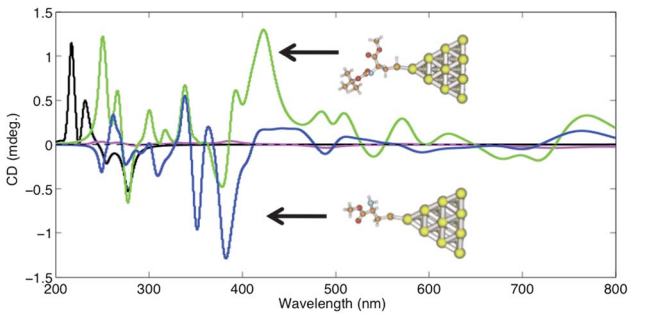


**Fig. 6** Calculated CD spectra of the free cysteine ester ligand molecule (black line), $Ag_{20}$ without a chiral ligand (magenta line), *t*-BOC protected $Ag_{20}$-cysteine ester complex (green line) and *t*-BOC deprotected $Ag_{20}$-cysteine ester complex (blue line).

optimized geometry for the $Ag_{20}$ cluster was taken from ref. 42. A triple-zeta Slater-type atomic orbital (STO) basis set with polarization functions (TZP) was used for all atoms. The spectra were broadened by a Lorentzian with a halfwidth of 0.2 eV. The results of these calculations are presented in Fig. 6. Chirality of the cysteine ester induces new red-shifted CD bands, not present in the ligand or silver cluster alone, which can be explained in the framework of our model by new chiral electronic states of the complexes. It is worth noting that one of the new CD bands is centered at the plasmon frequency, even though the modeled cluster is too small to exhibit a plasmon resonance.

## Conclusions

In summary, the optical chiral response of individual ligand-protected Ag NPs was successfully integrated into patterned films. The resulting CD response shows that there is a strong ligand-induced chirality at the plasmon frequency of Ag NPs. Moreover, CD bands at longer wavelengths, which are not present in solution, are observed in the films, due to the collective plasmon excitation of the coupled plasmonic NPs. These results show an enhancement of pre-tailored optical properties and suggest that our photopatternable Ag NPs can be useful for CD-based applications at visible wavelengths.[25,44] Moreover, this approach for patterning can enhance the optical activity of geometrically chiral structures, if one can pattern these chiral elements with dimensions small enough to be optically active in the visible. Overlap of the molecular/plasmonic response with the shape-induced response can lead to even greater overall optical activity.[45] The presented technique allows coupling of top-down patterning with intrinsically chiral materials without extrinsic additives. That is, we have shown a mechanism to write any 2D element (chiral or not chiral). Moreover, the two-photon lithography can potentially allow patterning of 3D elements. The simple and straightforward lithographic approach shown here with Ag NPs can potentially be useful in the fabrication of MNP-based optoelectronic devices and is extendable to other MNPs.

## Acknowledgements

This work was supported in part by a grant from the Air Force Office of Scientific Research (grant no. FA95500610398).

## Notes and references

1 D. B. Amabilino, in *Chirality at the Nanoscale: Nanoparticles, Surfaces, Materials and more*, Wiley-VCH, 2009.
2 L. He, E. A. Smith, M. J. Natan and C. D. Keating, *J. Phys. Chem. B*, 2004, **108**, 10973.
3 I. Fernandez-Corbaton, X. Vidal, N. Tischler and G. Molina-Terriza, *J. Chem. Phys.*, 2013, **138**, 214311.
4 A. Herrmann and K. Mullen, *Chem. Lett.*, 2006, **35**, 978.
5 A. Molinos-Gómez, M. Maymó, X. Vidal, D. Velasco, J. Martorell and F. López-Calahorra, *Adv. Mater.*, 2007, **19**, 3814.
6 J. R. Lakowicz, *Anal. Biochem.*, 2001, **298**, 1.
7 A. V. Zayats, I. I. Smolyaninov and A. A. Maradudin, *Phys. Rep.*, 2005, **408**, 131.
8 M. Righini, A. S. Zelenina, C. Girard and R. Quidant, *Nat. Phys.*, 2007, **3**, 477.
9 L. He, E. A. Smith, M. J. Natan and C. D. Keating, *J. Phys. Chem. B*, 2004, **108**, 10973.
10 P. N. Prasad, in *Nanophotonics*, John Wiley & Sons, New York, 2004.
11 A. V. Andreev, M. M. Nazarov, I. R. Prudnikov, A. P. Shkurinov and P. Masselin, *Phys. Rev. B: Condens. Matter Mater. Phys.*, 2004, **69**, 035403.
12 T. Li, H. G. Park, H.-S. Lee and S.-H. Choi, *Nanotechnology*, 2004, **15**, S660.
13 J. M. Slocik, A. O. Govorov and R. R. Naik, *Nano Lett.*, 2011, **11**, 701.
14 B. M. Maoz, R. Weegen, Z. Fan, A. O. Govorov, G. Ellestad, N. Berova, E. W. Meijer and G. Markovich, *J. Am. Chem. Soc.*, 2012, **134**, 17807.
15 M. Zhu, H. Qian, X. Meng, S. Jin, Z. Wu and R. Jin, *Nano Lett.*, 2011, **11**, 3963.
16 C. Gautier and T. Bürgi, *J. Am. Chem. Soc.*, 2008, **130**, 7077.
17 H. Xu, E. J. Bjerneld, M. Käll and L. Börjesson, *Phys. Rev. Lett.*, 1999, **83**, 4357.
18 J. W. Chou, K.-C. Lin, Y.-L. Lee, C.-T. Yuan, F.-K. Hsueh, H.-C. Shih, W.-C. Fan, C.-W. Luo, M.-C. Lin, W.-C. Chou and D.-S. Chuu, *Nanotechnology*, 2009, **20**, 305202.
19 M. Hentschel, M. Saliba, R. Vogelgesang, H. Giessen, A. P. Alivisatos and N. Liu, *Nano Lett.*, 2010, **10**, 2721.
20 H. Shen, P. Bienstman and B. Maes, *J. Appl. Phys.*, 2009, **106**, 073109.
21 P. Wang, L. Chen, R. Wang, Y. Ji, D. Zhai, X. Wu, Y. Liu, K. Chen and H. Xu, *Nanoscale*, 2013, **5**, 3889.
22 A. Kuzyk, R. Schreiber, Z. Fan, G. Pardatscher, E. M. Roller, A. Högele, F. C. Simmel, A. O. Govorov and T. Liedl, *Nature*, 2012, **483**, 311.
23 M. A. Holden and P. S. Cremer, *J. Am. Chem. Soc.*, 2003, **125**, 8074.
24 C. Zhou and A. M. Walker, *Langmuir*, 2006, **22**, 11420.
25 N. Meinzer, E. Hendry and W. L. Barnes, *Phys. Rev. B: Condens. Matter Mater. Phys.*, 2013, **88**, 041407(R).
26 W. J. Kim, X. Vidal, A. Baev, H. Lee, M. T. Swihart and P. N. Prasad, *Appl. Phys. Lett.*, 2011, **98**, 133110.
27 T. Baldacchini, A.-C. Pons, J. Pons, C. LaFratta, J. Fourkas, Y. Sun and M. Naughton, *Opt. Express*, 2005, **13**, 1275.
28 S. Maruo and T. Saeki, *Opt. Express*, 2008, **16**, 1174.
29 S. Shukla, E. P. Furlani, X. Vidal, M. T. Swihart and P. N. Prasad, *Adv. Mater.*, 2010, **22**, 3695.
30 S. Shukla, X. Vidal, E. P. Furlani, M. T. Swihart, K.-T. Kim, Y.-K. Yoon, A. Urbas and P. N. Prasad, *ACS Nano*, 2011, **5**, 1947.
31 J. Seo, W. J. Kim, S. J. Kim, K.-S. Lee, A. N. Cartwright and P. N. Prasad, *Appl. Phys. Lett.*, 2009, **94**, 133302.
32 I.-K. Shim, Y. I. Lee, K. J. Lee and J. Joung, *Mater. Chem. Phys.*, 2008, **110**, 316.

 

33 B.-h. Choi, H.-H. Lee, S. Jin, S. Chun and S.-H. Kim, *Nanotechnology*, 2007, **18**, 075706.
34 C. Gautier and T. Bürgi, *J. Am. Chem. Soc.*, 2006, **128**, 11079.
35 H. Tamaru, H. Kuwata, H. T. Miyazaki and K. Miyano, *Appl. Phys. Lett.*, 2002, **80**, 1826.
36 N. A. Abdulrahman, Z. Fan, T. Tonooka, S. M. Kelly, N. Gadegaard, E. Hendry, A. O. Govorov and M. Kadodwala, *Nano Lett.*, 2012, **12**, 977.
37 A. O. Govorov, Z. Fan, P. Hernandez, J. M. Slocik and R. R. Naik, *Nano Lett.*, 2010, **10**, 1374.
38 H. Zhang and A. O. Govorov, *Phys. Rev. B: Condens. Matter Mater. Phys.*, 2013, **87**, 075410.
39 J.-M. Ha, A. Solovyov and A. Katz, *Langmuir*, 2009, **25**, 153.
40 M. E. Layani, A. Ben Moshe, M. Varenik, O. Regev, H. Zhang, A. O. Govorov and G. Markovich, *J. Phys. Chem. C*, 2013, DOI: 10.1021/jp400993j.
41 Z. Rinkevicius, J. Autschbach, A. Baev, M. Swihart, H. Ågren and P. N. Prasad, *J. Phys. Chem. A*, 2010, **114**, 7590.
42 L. Zhao, L. Jensen and G. C. Schatz, *J. Am. Chem. Soc.*, 2006, **128**, 2911.
43 J. P. Perdew, K. Burke and Y. Wang, *Phys. Rev. B: Condens. Matter Mater. Phys.*, 1996, **54**, 16533.
44 A. Baev, M. Samoc, P. N. Prasad, M. Krykunov and J. A. Autschbach, *Opt. Express*, 2007, **15**, 5730.
45 E. P. Furlani, H. S. Jee, H. S. Oh, A. Baev and P. N. Prasad, *Adv. OptoElectron.*, 2012, **2012**, 861569.